

This is the accepted manuscript made available via CHORUS. The article has been published as:

Role of nuclear dynamics in the asymmetric molecular-frame photoelectron angular distributions for C 1s photoejection from CO₂

S. Miyabe, D. J. Haxton, T. N. Rescigno, and C. W. McCurdy

Phys. Rev. A **83**, 023404 — Published 4 February 2011

DOI: [10.1103/PhysRevA.83.023404](https://doi.org/10.1103/PhysRevA.83.023404)

Role of nuclear dynamics in the Asymmetric molecular-frame photoelectron angular distributions for C 1s photoejection from CO₂

S. Miyabe,^{1,2} D.J. Haxton,¹ T. N. Rescigno,¹ and C.W. McCurdy^{1,3}

¹*Lawrence Berkeley National Laboratory, Chemical Sciences and Ultrafast X-Ray Science Laboratory, Berkeley, CA 94720*

²*Department of Chemistry, University of California, Davis, CA 95616*

³*Departments of Chemistry and Applied Science, University of California, Davis, CA 95616*

We report the results of semiclassical calculations of the asymmetric molecular-frame photoelectron angular distributions for C 1s ionization of CO₂ measured with respect to the CO⁺ and O⁺ ions produced by subsequent Auger decay, and show how the decay event can be used to probe ultrafast molecular dynamics of the transient cation. The fixed-nuclei photoionization amplitudes were constructed using variationally obtained electron-molecular ion scattering wave functions. The amplitudes are then used in a semiclassical manner to investigate their dependence on the nuclear dynamics of the cation. The method introduced here can be used to study other core-level ionization events.

I. INTRODUCTION

The the process of photoionization and subsequent Auger decay has long been used to study phenomena in physics and chemistry. In brief, photoionization of a core electron leaves a molecule in a highly excited state. Since it is unstable, it can undergo an Auger process by filling the created hole with one of the valence electrons, while another valence electron gets ejected from the molecule. It is expected that the lifetime and the molecular dynamics of the transient molecule will have a strong influence on the measured quantities. To compute cross sections to analyze these complex experimental measurements, a method that accounts for the dynamics of the photoionized molecule is needed.

Recently, Liu *et al.*[1] and Sturm *et al.*[2] have shown that the molecular-frame photoelectron angular distribution (MFPAD) for C 1s ionization of CO₂ is asymmetric with respect to CO⁺ + O⁺ fragment ions for certain photon energies. Liu *et al.* speculated that the asymmetry results from an interference between gerade and ungerade intermediate states, implying a partial breakdown of the two-step model for photoionization and Auger decay. In contrast, we have previously shown that the asymmetry can be explained from the knowledge of the photoionization event alone if we consider the nuclear dynamics of the transient cation and the time scale of the Auger decay [3]. We proposed a mechanism to explain how the memory of the photoelectron angular distributions produced from asymmetric nuclear geometries is imprinted on the nuclear dynamics following Auger decay. Since the Auger lifetime is shorter than the asymmetric stretch vibrational period, population of an electronically excited dication state that produces CO⁺ + O⁺ fragment ions by direct dissociation can be used to monitor any asymmetry in the photoelectron angular distribution when measured in coincidence with the latter. In this manner, we showed how the Auger decay and fragmentation can be used to probe ultrafast molecular dynamics of the transient CO₂⁺.

However, in our previous calculation, we assumed that the Auger decay was an instantaneous process, and we

did not explicitly take the molecular dynamics of the transient cation into account. Thus, the asymmetry was overestimated compared with the experiment. Here, we present a semiclassical approach that accounts for the molecular dynamics of the core-hole ionized state, and provide more proof for our proposed mechanism. The calculated MFPAD gives a good agreement with the measurement of Liu *et al.*. Furthermore, the method developed here can be used to study other core-level ionization events.

II. THEORY

A. Computation of molecular-frame photoionization cross sections

Fixed-nuclei photoionization amplitudes were computed using the complex Kohn variational method [4]. Here we give a brief summary. The final-state wave function for production of photoions in a specific cation state Γ_0 and with final angular momentum $l_0 m_0$ is written as

$$\Psi_{\Gamma_0 l_0 m_0}^- = \sum_{\Gamma m} A(\chi_{\Gamma} F_{\Gamma m \Gamma_0 l_0 m_0}^-) + \sum_i d_i^{\Gamma_0 l_0 m_0} \Theta_i \quad (1)$$

where Γ labels the final ionic target states χ_{Γ} included, F^- are channel functions that describe the photoionized electron, A is the antisymmetrization operator and the Θ_i 's are N electron correlation terms. In the present application, only one ionic target state is included in the trial wave function, that being the C(1s⁻¹) hole state.

In the Kohn method, the channel functions are further expanded, in the molecular frame, as

$$\begin{aligned} F_{\Gamma m \Gamma_0 l_0 m_0}^- (\mathbf{r}) = & \sum_i c_i^{\Gamma m \Gamma_0 l_0 m_0} \varphi_i(\mathbf{r}) \\ & + \sum_{lm} \left[f_{lm}(k_{\Gamma}, r) \delta_{ll_0} \delta_{mm_0} \delta_{\Gamma \Gamma_0} \right. \\ & \left. + T_{l_0 m m_0}^{\Gamma \Gamma_0} h_{lm}^-(k_{\Gamma}, r) \right] Y_{lm}(\hat{\mathbf{r}}) / k_{\Gamma}^{\frac{1}{2}} r, \end{aligned} \quad (2)$$

where the $\varphi_i(\mathbf{r})$ are a set of square-integrable (Cartesian Gaussian) functions, Y_{lm} is a normalized spherical harmonic, k_Γ are channel momenta, and the $f_{lm}(k_\Gamma, \mathbf{r})$ and $h_{lm}^-(k_\Gamma, \mathbf{r})$ are numerical continuum functions that behave asymptotically as regular and incoming partial-wave Coulomb functions, respectively [5]. The coefficients $T_{l_0 m_0}^{\Gamma \Gamma_0}$ are the T-matrix elements.

Photoionization cross sections in the molecular frame can be constructed from the matrix elements

$$I_{\Gamma_0 l_0 m_0}^\mu = \langle \Psi_{\Gamma_0 l_0 m_0}^- | r_\mu | \Psi_0 \rangle, \quad (3)$$

where r_μ is a component of the dipole operator, which we evaluate here in the length form,

$$r_\mu = \begin{cases} z, & \mu = 0 \\ \mp (x \pm iy) / \sqrt{2}, & \mu = \pm 1 \end{cases} \quad (4)$$

and Ψ_0 is the initial state wave function of the neutral N electron target. In order to construct an amplitude that represents a photoelectron with momentum \mathbf{k}_{Γ_0} ejected by absorption of a photon with polarization direction $\hat{\epsilon}$, measured relative to the molecular body-frame, the matrix elements $I_{\Gamma_0 l_0 m_0}^\mu$ must be combined in a partial wave series

$$I_{\hat{k}, \Gamma_0, \hat{\epsilon}} = \sqrt{\frac{4\pi}{3}} \sum_{\mu l_0 m_0} i^{-l_0} e^{i\delta_{l_0}} I_{\Gamma_0 l_0 m_0}^\mu Y_{1\mu}(\hat{\epsilon}) Y_{l_0 m_0}(\hat{k}), \quad (5)$$

where δ_{l_0} is a Coulomb phase shift. The cross section, differential in the angle of photoejection and photon polarization relative to the fixed body-frame of the molecule, is then given by

$$\frac{d^2\sigma}{d\Omega_{\hat{k}} d\Omega_{\hat{\epsilon}}} = \frac{8\pi\omega}{3c} |I_{\hat{k}, \Gamma_0, \hat{\epsilon}}|^2, \quad (6)$$

where ω is the photon energy and c is the speed of light.

B. Inclusion of vibrational motion

To account for the target vibrational motion, we make the Born-Oppenheimer approximation for the initial state and the final scattering states, writing them as products of electronic and vibrational functions. We can then rewrite the amplitude (defined in Eq. 5) for a particular $\nu \rightarrow \nu'$ transition as

$$I_{\hat{k}, \Gamma_0, \hat{\epsilon}}^{\nu, \nu'} = \sqrt{\frac{4\pi}{3}} \sum_{\mu l_0 m_0} i^{-l_0} e^{i\delta_{l_0}} Y_{1\mu}(\hat{\epsilon}) Y_{l_0 m_0}(\hat{k}) \times \int I_{\Gamma_0 l_0 k_0}^\mu(\mathbf{s}) \eta_\nu(\mathbf{s}) \eta_{\nu'}(\mathbf{s}) d\mathbf{s}, \quad (7)$$

where we have used \mathbf{s} to denote the internal coordinates and η_ν and $\eta_{\nu'}$ are the initial (neutral) and final (ion) vibrational wave functions, respectively. Note that we

have ignored the dependence of the photoelectron wave vector \mathbf{k} on the final vibrational state, which is a good approximation except very close to thresholds. If we are not interested in the excitation of individual vibrational levels, then we can sum over final ν' in computing the body-frame cross section, using the closure relation,

$$\sum_{\nu'} \eta_{\nu'}(\mathbf{s}) \eta_{\nu'}(\mathbf{s}') = \delta(\mathbf{s} - \mathbf{s}') \quad (8)$$

to obtain the differential body-frame photoionization cross section for a target molecule in initial vibrational state ν

$$\frac{d^2\sigma_\nu}{d\Omega_{\hat{k}} d\Omega_{\hat{\epsilon}}} = \int \eta_\nu(\mathbf{s})^2 \frac{d^2\sigma}{d\Omega_{\hat{k}} d\Omega_{\hat{\epsilon}}}(\mathbf{s}) d\mathbf{s}. \quad (9)$$

Note that we approximate the initial vibrational wave function as a product of harmonic oscillator functions in the asymmetric-stretch and bending normal coordinates using force constants derived from our SCF calculations. We found that averaging over symmetric-stretch motion had little effect on the angular distributions, so the results we present include only asymmetric-stretch and bending. Bending motion does not of course break the left/right symmetry of the molecule, but improves the quantitative agreement between calculated and measured angular distributions.

C. Semiclassical approximation

We begin with the brief description of the process. The C 1s photoejection of CO_2 will leave the molecule in a highly excited state. The CO_2^+ formed in this manner is very unstable and, on average, it Auger decays within ~ 6 fs to make the Auger electron and the dication. The Auger process can feed a number of final dication channels. Of the possible final dication channels, one or more involve prompt fragmentation directly into $\text{O}^+ + \text{CO}^+$ so that the axial recoil approximation is valid. We have previously shown that $3^1\Pi$ state of the dication leads to such fragmentation [3]. In the COLTRIMS experiment, the body-frame photoelectron angular distributions are measured in coincidence with this asymmetric ion fragmentation.

We previously demonstrated that the nuclear dynamics of the cation during the Auger lifetime plays a significant role in the observed asymmetric photoelectron angular distribution without explicitly taking the decay process into consideration. In order to observe the asymmetry, the Auger decay must take place before the molecular ion can exert enough vibrational motion that would erase the memory of the geometry at which it was created. In accordance with our proposed mechanism, if Auger decay was instantaneous, we could integrate Eq. 9 over half of the allowed nuclear geometries in the asymmetric stretch coordinate and obtain the desired result. However, the Auger lifetime is finite, and as a consequence, the asymmetry is expected to be washed away to a certain extent

by the nuclear motion. At the other extreme, if the lifetime of the cation is comparable to the asymmetric mode period, ~ 14.2 fs, we would expect symmetric distributions.

We can modify Eq. 9 with a semiclassical model that incorporates the effect of finite Auger lifetime into the calculation. We define the MFPAD, for observing the CO^+ going to the left, is as

$$\left(\frac{d^2\sigma_\nu}{d\Omega_{\hat{k}} d\Omega_{\hat{\epsilon}}} \right)_L = \int_{-\infty}^{\infty} ds_B \int_{-\infty}^{\infty} ds_A \eta_\nu(s_B)^2 \eta_\nu(s_A)^2 \times \frac{d^2\sigma}{d\Omega_{\hat{k}} d\Omega_{\hat{\epsilon}}}(s_B, s_A) \int dt P(t) \theta(q(s_A, t)), \quad (10)$$

where s_B and s_A are the normal coordinates in the bending and asymmetric stretch modes, respectively, t is the time of decay, $P(t)$ is the probability per unit time to decay at time t , $q(s_A, t)$ is the classical trajectory of the nuclei, which describes the nuclear motion of CO_2^+ in its transient C 1s core-hole state, and $\theta(s_A)$ is a heaviside function, which is zero for $s_A < 0$ and one for $s_A \geq 0$. Note that $q(s_A, t)$ is a function of time and the asymmetric stretch coordinate only since we assume the bending motion does not influence the left/right asymmetry.

The probability per unit time for the cation to decay at time t is given by

$$P(t) = \Gamma \exp(-\Gamma t), \quad (11)$$

Using the above expressions, Eq. 10 becomes

$$\begin{aligned} \left(\frac{d^2\sigma_\nu}{d\Omega_{\hat{k}} d\Omega_{\hat{\epsilon}}} \right)_L &= \int_{-\infty}^{\infty} ds_B \eta_\nu(s_B)^2 \left(P_{\text{switch}} \int_{-\infty}^0 ds_A + P_{\text{stay}} \int_0^{\infty} ds_A \right) \eta_\nu(s_A)^2 \frac{d^2\sigma}{d\Omega_{\hat{k}} d\Omega_{\hat{\epsilon}}}(\mathbf{s}) \\ &= P_{\text{switch}} \sigma_{\text{sym}} + (P_{\text{stay}} - P_{\text{switch}}) \int_{-\infty}^{\infty} ds_B \int_0^{\infty} ds_A \eta_\nu(s_B)^2 \eta_\nu(s_A)^2 \frac{d^2\sigma}{d\Omega_{\hat{k}} d\Omega_{\hat{\epsilon}}}(\mathbf{s}). \end{aligned} \quad (15)$$

where σ_{sym} is the Franck-Condon average of the MFPAD:

$$\sigma_{\text{sym}} = \int_{-\infty}^{\infty} ds_B \int_{-\infty}^{\infty} ds_A \eta_\nu(s_B)^2 \eta_\nu(s_A)^2 \frac{d^2\sigma}{d\Omega_{\hat{k}} d\Omega_{\hat{\epsilon}}}(s_B, s_A). \quad (16)$$

Note that Eq. 15 reduces to Eq. 9 in the limit Auger decay is instantaneous.

III. RESULTS

The square-integrable portion of the basis for the complex Kohn calculations consisted of Dunning's double-zeta basis [7], augmented with two p-type, two d-type and three f-type functions on the carbon atom, along with two p-type, two d-type and one f-type function on the oxygen atoms. We also included numerical continuum functions up to $l=7$. To avoid working with non-

where Γ is the Auger width (99 meV [6]).

We approximate the potential energy surface of CO_2^+ along asymmetric stretch as a harmonic oscillator potential with the same angular frequency ω as neutral CO_2 , which can be derived from its IR frequency. Then the classical trajectory is

$$s_A(t) = S_A \cos \omega t. \quad (12)$$

The time integral for $s_A < 0$, which is the probability that the CO_2^+ trajectory starts with a CO bond compressed on one side of the molecule and decays with a CO bond compressed on the other side, is

$$\begin{aligned} &\int dt \Gamma \exp(-\Gamma t) \theta(-S_A \cos \omega t) \\ &= \frac{\exp(-\pi\omega\Gamma)}{1 + \exp(-2\pi\omega\Gamma)} \equiv P_{\text{switch}}. \end{aligned} \quad (13)$$

P_{stay} , the probability of decaying on the same side as the start of the trajectory is then,

$$P_{\text{stay}} = \int dt \Gamma \exp(-\Gamma t) \theta(S_A \cos \omega t) = 1 - P_{\text{switch}}. \quad (14)$$

orthogonal orbitals, we use a single set of molecular orbitals to construct both the initial neutral and final ion states. In order to generate these orbitals, we start with a reference ion configuration with a single vacancy in the carbon 1s orbital. We then perform an all-singles configuration-interaction calculation, keeping the carbon 1s occupancy either one or zero. The natural orbitals from that calculation, obtained by diagonalizing the one-particle density matrix, are then used in the second set of photoionization calculations.

Fig. 1 shows the MFPADs computed using the semiclassical approach given by Eq. 15. The black dotted line in Fig. 1a shows the molecular-frame photoelectron an-

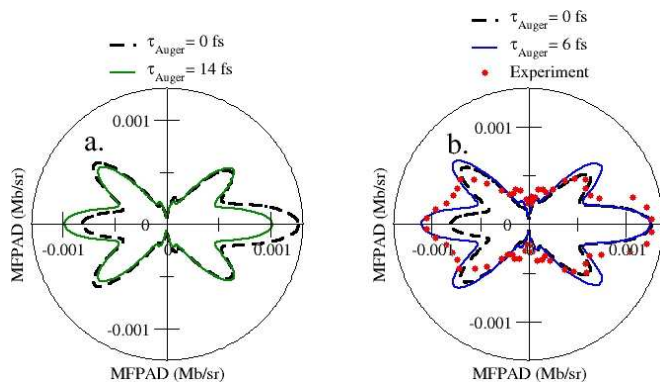


FIG. 1: (Color online) a). Molecular-frame photoelectron angular distribution of CO₂ computed with Auger lifetime set at 0 fs (black dotted curve) and 14 fs (green solid line). b). MFPAD calculated for Auger lifetime set to 0 fs (black dotted curve) and 6 fs (solid blue curve) along with the experimental result shown in red dots. Note that the magnitude of the cross sections are normalized at $\theta_{\text{photo-e}} = 0$ degrees.

gular distribution calculated assuming the Auger decay to be instantaneous. It shows a significant asymmetry. Note that this is identical to the result presented in our previous study[3]. On the other extreme, if the Auger lifetime is comparable to the period of asymmetric vibrational motion, the asymmetry is completely washed away. This is shown as the green solid curve in Fig. 1a. Fig. 1b compares the computed MFPAD to the exper-

imental one[1]. Note that the magnitude of the cross sections are normalized at $\theta_{\text{photo-e}} = 0$ degrees. Clearly, the nuclear dynamics during the Auger lifetime of the cation is very important in reproducing the experimental result. If we assume the Auger lifetime, τ_{Auger} , to be 0 fs, the asymmetry is overestimated (black dotted curve). Using the experimental value of the Auger decay width, the agreement between the observed and the calculated becomes very good (blue solid curve). The affect of postcollision interaction between the photoelectron and the Auger electron is not included in this calculation. Thus, these results show that the asymmetry in the photoelectron angular distribution can be completely explained without any knowledge of the subsequent Auger decay step. This demonstrates the validity of the two-step model in the coincident measurement of photoelectron with fragment ions produced following Auger decay.

Acknowledgments

This work was performed under the auspices of the US Department of Energy by the University of California Lawrence Berkeley National Laboratory under Contract DE-AC02-05CH11231 and was supported by the U.S. DOE Office of Basic Energy Sciences, Division of Chemical Sciences. CWM acknowledges support from the National Science Foundation (Grant No. PHY-0604628).

-
- [1] X.-J. Liu, H. Fukuzawa, T. Teranishi, A. De Fanis, M. Takahashi, H. Yoshida, A. Cassimi, A. Czasch, L. Schmidt, R. Dörner, K. Wang, B. Zimmermann, V. McKoy, I. Koyano, N. Saito, and K. Ueda, *Phys. Rev. Lett.* **101**, 083001 (2008).
 - [2] F. P. Sturm, M. Schöffler, S. Lee, T. Osipov, N. Neumann, H.-K. Kim, S. Kirschner, B. Rudek, J. B. Williams, J. D. Daughhetee, C. L. Cocke, K. Ueda, A. L. Landers, T. Weber, M. H. Prior, A. Belkacem, and R. Dörner, *Phys. Rev. A* **80**, 032506 (2009).
 - [3] S. Miyabe, C. W. McCurdy, A. E. Orel, and T. N. Rescigno, *Phys. Rev. A* **79**, 053401 (2009).
 - [4] T. N. Rescigno, B. H. Lengsfeld, and C. W. McCurdy, in *Modern Electronic Structure Theory*, edited by D. R. Yarkony (World Scientific, Singapore, 1995), Vol. 1.
 - [5] T. N. Rescigno and A. E. Orel, *Phys. Rev. A* **43**, 1625–1628 (1991).
 - [6] T. X. Carroll, J. Hahne, T. D. Thomas, L. J. Sæthre, N. Berrah, J. Bozek, and E. Kukk, *Phys. Rev. A* **61**, 042503 (2000).
 - [7] T. H. Dunning, *Journal of Chemical Physics* **53**, 2823 (1970).